INT. J. NUM. METH. HEAT FLUID FLOW, VOL. 6, 59–77 (1996)

SOLUTION OF STEADY INVISCID SUBSONIC FLOW BY A LOCALLY ANALYTIC METHOD

MATTHEW MONTGOMERY AND SANFORD FLEETER

Thermal Sciences and Propulsion Center, School of Mechanical Engineering Purdue University, West Lafayette, Indiana 47907, USA

ABSTRACT

The first compressible flow solution based solely on the locally analytical method is developed. This is accomplished by developing the flow model and locally analytical solution for inviscid subsonic compressible flow. The stream function for irrotational, compressible flow without body forces was chosen as the governing differential equation. To demonstrate the modelling and locally analytical solution, this analysis is then applied to predict the flow in convergent nozzles, both planar and axially symmetric, for different back pressures. Results are presented which demonstrate the effectiveness of this technique.

KEY WORDS Subsonic Inviscid flow Locally analytical solution Convergent nozzles

NOMENCLATURE

a	local sound speed	q_n	normal velocity in streamline coordinates
$\hat{a}$	non-dimensional sound speed, a/a^*	r	over-relaxation factor
a^*	critical sound speed	s	streamwise direction in streamline coordinates
a_0	stagnation sound speed	u	velocity in x direction
A	cross sectional area, coefficient of linearized equation	$\hat{u}$	non-dimensional velocity in x direction, u/a^*
A^*	critical cross sectional area	v	velocity in y direction
h	grid spacing in computational plane	$\hat{v}$	non-dimensional velocity in y direction, v/a^*
i, j	grid indices	V	velocity magnitude
M	Mach number, V/a	$\vec{V}$	velocity vector
n	normal direction in streamline coordinates	x	streamwise direction
p	static pressure	y	normal or radial direction
$\hat{p}$	non-dimensional pressure, p/P_0	ρ	static density
p_{back}	exit plane back pressure	$\hat{\rho}$	nom-dimensional density, ρ/ρ_0
P_0	stagnation pressure	ρ_0	stagnation density
q	velocity in streamline coordinates	ψ	stream function

INTRODUCTION

There have been many advances in the analysis and prediction of fluid flow phenomena due, in part, to the continuing development of finite difference and element methods and the introduction of new numerical techniques, of particular interest herein being the locally analytical method.

The various numerical methods utilized to solve partial differential equations are distinguished from one another by the means used to derive the corresponding algebraic representation of the differential equations. In finite difference methods, Taylor series expansion and control volume

0961–5539/96/010059–19$2.00

Received October 1994

formulations are most often used. For finite element methods, variational formulations and the method of weighted residuals are employed. In the locally analytical method, the discrete algebraic equations are obtained from the analytical solution in each individual local grid element.

The locally analytical method, developed by Chen[1,2], uses the solution of the governing equation, locally linearized in each computational cell, to construct the approximate solution. In contrast, finite difference and finite element methods typically use low order polynomials in the computational cells to approximate the solution. The locally analytical method is a relaxation, as opposed to marching, method. Each node is defined in terms of its neighbours, with the coefficients determined by the linearized governing equation. The method is thus limited to elliptic and parabolic problems with unlimited domains of dependence. In this investigation, subsonic flow is considered, resulting in an elliptic problem.

The overall objective of this research is the development of the first compressible flow solution based solely on the locally analytic method. Chen[3] used a type of locally analytic method for steady, two-dimensional, supersonic flow but this was a modification of the inverse marching method of characteristics. Naixing[4] solved for the steady, two-dimensional, subsonic flow in a turbine cascade with the locally analytic method, but apparently also used finite difference techniques to solve the continuity equation. The method presented here relies solely on the locally analytic method for the solution of the stream function and its derivatives.

In this paper, the modelling and locally analytical solution are developed for inviscid subsonic compressible flow. The governing equations are developed in a form amenable to numerical solution. The stream function for irrotational, compressible flow without body forces was chosen as the governing differential equation. With the simplifying assumptions made the remaining governing equations reduce to algebraic equations. To demonstrate the modelling and locally analytical solution, this analysis is then applied to predict the flow in convergent nozzles, both planar and axially symmetric, for different back pressures. Results are then presented which demonstrate the effectiveness of this technique.

GOVERNING EQUATIONS

The fluid is assumed to be a perfect gas with zero viscosity and thermal conductivity. Body forces are ignored and the motion is assumed to be steady and two dimensional. The adiabatic, isentropic planar or axisymmetric flow is considered to originate from a reservoir with uniform stagnation conditions. The variables defining the flow field are the stream function, pressure and density. Pressure and density are related algebraically through the equation of state, the homentropic condition, and the sound speed. The sound speed equation is then related to the derivatives of the stream function. Thus solving the stream function equation completely determines the flow field.

The governing equation for the stream function is developed by combining the irrotationality condition, the equation of motion, and the sound speed in streamline coordinates. In this system the s direction is the direction of the velocity and the n direction is normal to the velocity as defined by the right hand rule. The velocity magnitude is denoted by q, with q_n the velocity in the normal direction. Although q_n is identically zero, the derivatives of q_n are nonzero.

The planar and axially symmetric stream functions are given in (1):

$$[u^2-a^2]\frac{\partial^2\psi}{\partial x^2}+[v^2-a^2]\frac{\partial^2\psi}{\partial y^2}+2uv\frac{\partial^2\psi}{\partial x\partial y}=0 \tag{1a}$$

$$[u^2-a^2]\frac{\partial^2\psi}{\partial x^2}+[v^2-a^2]\frac{\partial^2\psi}{\partial y^2}+2uv\frac{\partial^2\psi}{\partial x\partial y}=-\frac{a^2}{y}\frac{\partial\psi}{\partial y} \tag{1b}$$

The pressure and density are non-dimensionalized with their respective stagnation values while

all velocities are made dimensionless with the critical sound speed, a^*.

$$\hat{p}=\frac{p}{P_0}=\hat{\rho}^{\gamma} \tag{2}$$

$$\hat{\rho}=\frac{\rho}{\rho_0}=\left(\frac{2\hat{a}^2}{\gamma+1}\right)^{1/(\gamma-1)} \tag{3}$$

$$\hat{a}^2=\frac{a}{a^*}=0.5[\gamma+1+(1-\gamma)\hat{V}^2] \tag{4}$$

The flow problem to be solved by the locally analytical method is specified by (1) through (4).

NOZZLE GEOMETRY

The subsonic flow through a converging nozzle is considered. The nozzle wall is specified in (5), with $y=0$ defining the centreline and x varying from 0 to 1. Since the exist wall slope is zero, the exit flow is a uniform jet,

$$y=(3+\cos(\pi x))/8 \tag{5}$$

An algebraic grid is used to transform the nozzle into the orthogonal computational plane. The streamwise grid lines are positioned by a linear stretching function, H, that varies with the nozzle height, (6), with (7) defining the normal transformation used to cluster grid lines near the nozzle throat, *Figure 1*,

$$\eta=yH(x) \tag{6}$$

$$\xi=sx^2 \tag{7}$$

where s is a scaling constant.

For subsonic flow, three boundary conditions are required at the upstream boundary and one at the downstream boundary. Upstream, the stagnation pressure and stagnation density are specified along with the flow angle set by defining the y-component of velocity to be zero. Downstream, the static pressure is specified,

$$P_0=1 \text{ at inlet} \tag{8a}$$

$$\rho_0=1 \text{ at inlet} \tag{8b}$$

$$v=0 \text{ at inlet} \tag{8c}$$

$$p=p_{back} \text{ at exit} \tag{8d}$$

The stream function is specified as constant along the nozzle centreline and wall. At the centreline the stream function is defined as zero and its values at the nozzle wall, inlet and outlet

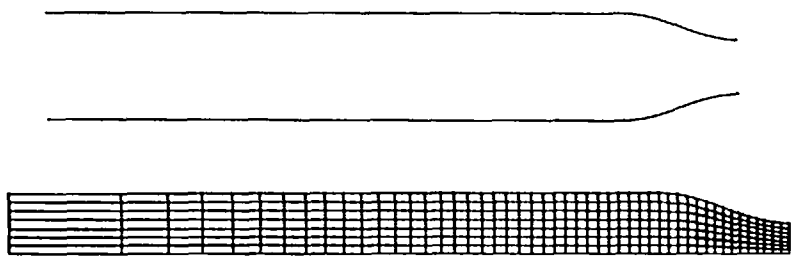

Figure 1 Nozzle geometry and grid

are computed by integrating the mass flux. These Dirichlet boundary conditions for the stream function lead to a straightforward iterative solution scheme, described in the following section.

SOLUTION PROCEDURE

The locally analytical solution is developed, including locally analytical expressions for the stream function and its derivatives. Next, the initialization procedure is described. Finally, the iteration procedure is described and the velocities at the boundaries are considered.

Locally analytical solution

The expression for the planar stream function is rearranged to yield (9), with a similar equation obtained by rearranging the axisymmetric stream function given in (1b).

$$\frac{\partial^2\psi}{\partial x^2}+\frac{[v^2-a^2]}{[u^2-a^2]}\frac{\partial^2\psi}{\partial y^2}=\frac{-2uv}{[u^2-a^2]}\frac{\partial^2\psi}{\partial x\partial y} \tag{9}$$

This equation is then written in the coordinate system defined by (6) and (7), with the velocities and cross derivatives in the coefficients evaluated and treated as constants. The governing equation is thus a general second-order partial differential equation of the following form,

$$\psi_{xx}+C\psi_{yy}-2A\psi_x-2BC\psi_y=f \tag{10}$$

where subscripts denote partial derivatives and A, B, C and f are taken as constants.

The flow field being analyzed is subsonic. Thus the constant C is positive and (10) is elliptic. The original solution of this equation is due to Chen[5].

Stream function solution

Equation (10) is solved in an evenly spaced rectangular domain. The value of the function at the origin, (x_i, y_j), is determined in terms of the values at the eight neighbouring nodes and the source term, f.

A change of variables is introduced to make the equation homogeneous,

$$\bar{\phi}=\psi+\frac{f(Ax+By)}{2(A^2+B^2C)} \tag{11}$$

where: $\phi=\bar{\phi}\exp(-Ax-By)$.

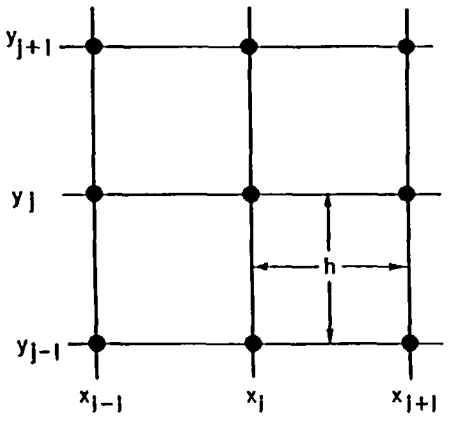

Figure 2 Computational grid cell

These change (10) to the following form. Note that the variable ϕ is not the potential function,

$$\phi_{xx}+C\phi_{yy}-\phi(A^2+B^2C)=0 \tag{12}$$

The boundary conditions for the computational cell shown in *Figure 2* are constructed from the particular solution to (10). These particular solutions are constant, linear and exponential functions. The boundary function for the y_{j+1} boundary is defined in (13).

$$\bar{\phi}_{j+1}(x)=a_{j+1}[\exp(2Ax)-1]+xb_{j+1}+c_{j+1} \tag{13}$$

where,

$$a_{j+1}=\frac{\bar{\phi}_{i+1,j+1}+\bar{\phi}_{i-1,j+1}-2\bar{\phi}_{i,j+1}}{4\sinh^2(Ah)}$$

$$b_{j+1}=\frac{\bar{\phi}_{i+1,j+1}-\bar{\phi}_{i-1,j+1}-[\bar{\phi}_{i+1,j+1}+\bar{\phi}_{i-1,j+1}-2\bar{\phi}_{i,j+1}]\coth(Ah)}{2h}$$

$$c_{j+1}=\bar{\phi}_{i,j+1}$$

In these definitions, A is the constant from (10) and h is the grid spacing in the computational plane. The boundary functions for the y_{j-1}, x_{i+1} and x_{i-1} boundaries are similar.

In terms of the variable ϕ, the boundary functions are:

$$\phi_{j+1}(x)=\exp(-Bh)[a_j+1\exp(Ax)+xb_{j+1}\exp(-Ax)+(c_{j+1}-a_{j+1})\exp(-Ax)] \tag{14a}$$

$$\phi_{j-1}(x)=\exp(Bh)[a_{j-1}\exp(Ax)+xb_{j-1}\exp(-Ax)+(c_{j-1}-a_{j-1})\exp(-Ax)] \tag{14b}$$

$$\phi_{i+1}(y)=\exp(-Ah)[a_{i+1}\exp(By)+yb_{i+1}\exp(-By)+(c_{i+1}-a_{i+1})\exp(-By)] \tag{14c}$$

$$\phi_{i-1}(y)=\exp(Ah)[a_{i-1}\exp(By)+yb_{i-1}\exp(-By)+(c_{i-1}-a_{i-1})\exp(-By)] \tag{14d}$$

The problem for ϕ thus consists of a linear differential equation and four inhomogeneous boundary conditions. The solution is developed by considering four component problems, (15), each of which has three homogeneous boundary conditions and one inhomogeneous condition. Superposition allows these component problems to be summed to give the solution to the original problem. These four component problems are specified in (16) through (19),

$$\phi(x,\,y)=\phi_1(x,\,y)+\phi_2(x,\,y)+\phi_3(,\,y)+\phi_4(x,\,y) \tag{15}$$

ϕ_1:

$$\phi_{j+1}(x)=\exp(-Bh)[a_{j+1}\exp(Ax)+xb_{j+1}\exp(-Ax)+(c_{j+1}-a_{j+1})\exp(-Ax)] \tag{16a}$$

$$\phi_{j-1}(x)=0 \tag{16b}$$

$$\phi_{i+1}(y)=0 \tag{16c}$$

$$\phi_{i-1}(y)=0 \tag{16d}$$

ϕ_2:

$$\phi_{j+1}(x)=0 \tag{17a}$$

$$\phi_{j-1}(x)=\exp(+Bh)[a_{j-1}\exp(Ax)+xb_{j-1}\exp(-Ax)+(c_{j-1}-a_{j-1})\exp(-Ax)] \tag{17b}$$

$$\phi_{i+1}(y)=0 \tag{17c}$$

$$\theta_{i-1}(y)=0 \tag{17d}$$

ϕ_3:

$$\phi_{j+1}(x)=0 \tag{18a}$$

$$\phi_{j-1}(x)=0 \tag{18b}$$

$$\phi_{i+1}(y)=\exp(-Ah)[a_{i+1}\exp(By)+yb_{i+1}\exp(-By)+(c_{i+1}-a_{i+1})\exp(-By)] \tag{18c}$$

$$\phi_{i-1}(y)=0 \tag{18d}$$

ϕ_4:

$$\phi_{j+1}(x)=0 \tag{19a}$$

$$\phi_{j-1}(x)=0 \tag{19b}$$

$$\phi_{i+1}(y)=0 \tag{19c}$$

$$\phi_{i-1}(y)=\exp(+Ah)[a_{i-1}\exp(By)+yb_{i-1}\exp(-By)+(c_{i-1}-a_{i-1})\exp(-By)] \tag{19d}$$

Equation (12) is solved by separation of variables. Letting ϕ denote the product of two single variable functions, (20), leads to (21),

$$\phi(x, y)=\xi(x)\eta(y) \tag{20}$$

$$-\frac{\xi_{xx}}{\xi}+A^2+B^2C=C\frac{\eta_{yy}}{\eta}=-\lambda \tag{21}$$

where λ is a separation constant.

For the ϕ_1 and ϕ_2 problems, (21) is used in the following form,

$$\xi_{xx}+\lambda\xi=0 \tag{22a}$$

$$\eta_{yy}-(\lambda+A^2+B^2C)\eta/C=\eta_{yy}-\omega^2\eta=0 \tag{22b}$$

Equation (22b) defines the parameter ω. Solution of this Sturm-Liouville problem leads to the following eigenvalues and eigenfunctions:

$$\lambda_n=\alpha_n^2=\left(\frac{n\pi}{2h}\right)^2 \qquad \text{where } n=1, 2, 3, \ldots \tag{23a}$$

$$\xi_{1n}=\xi_{2n}=\sin[\alpha_n(x+h)] \tag{23b}$$

$$\eta_{1n}=\sinh[\omega_n(y+h)] \tag{23c}$$

$$\eta_{2n}=\sinh[\omega_n(y-h)] \tag{23d}$$

where:

$$\phi_1=\sum_{n=1}^{\infty} b_{1n}\xi_{1n}\eta_{1n}=\sum_{n=1}^{\infty} b_{1n}\sin[\alpha_n(x+h)]\sinh[\omega_n(y+h)] \tag{24a}$$

$$\phi_2=\sum_{n=1}^{\infty} b_{2n}\xi_{2n}\eta_{2n}=\sum_{n=1}^{\infty} b_{2n}\sin[\alpha_n(x+h)]\sinh[\omega_n(y-h)] \tag{24b}$$

$$b_{1n}=\frac{1}{h\sinh(2\omega_n h)}\int_{-h}^{+h}\phi_{j+1}(x)\sin[\alpha_n(x+h)]\,dx \tag{25a}$$

$$b_{2n}=\frac{1}{h\sinh(-2\omega_n h)}\int_{-h}^{+h}\phi_{j-1}(x)\sin[\alpha_n(x+h)]\,dx \tag{25b}$$

For the ϕ_3 and ϕ_4 component problems, (22b) is used in the following form,

$$C\eta_{yy}+\lambda\eta=0 \tag{26a}$$

$$\xi_{xx}-(\lambda+A^2+B^2C)\xi=\xi_{xx}-(\omega')^2\xi=0 \tag{26b}$$

Equation (26b) defines the parameter ω', with the solution of this Sturm-Liouville problem

leading to the following eigenvalues and eigenfunctions,

$$\frac{\lambda_n}{C}=\alpha_n^2=\left(\frac{n\pi}{2h}\right)^2 \qquad \text{where } n=1, 2, 3, \ldots \tag{27a}$$

$$\eta_{3n}=\eta_{4n}=\sin[\alpha_n(y+h)] \tag{27b}$$

$$\xi_{3n}=\sinh[\omega_n'(x+h)] \tag{27c}$$

$$\xi_{4n}=\sinh[\omega_n'(x.h)] \tag{27d}$$

The general solution is again obtained by summing over all of these solutions,

$$\phi_3=\sum_{n=1}^{\infty} b_{3n}\xi_{3n}\eta_{3n}=\sum_{n=1}^{\infty} b_{3n}\sin[\alpha_n(y+h)]\sinh[\omega_n'(x+h)] \tag{28a}$$

$$\phi_4=\sum_{n=1}^{\infty} b_{4n}\xi_{4n}\eta_{4n}=\sum_{n=1}^{\infty} b_{4n}\sin[\alpha_n(y+h)]\sinh[\omega_n'(x-h)] \tag{28b}$$

where b_{3n} and b_{4n} are calculated in a fashion similar to b_{1n} and b_{2n} (25).

The integration of (25a) makes use of several identities derivable from the real and imaginary parts of the following integral,

$$I=\int \exp(ax)\exp(ibx)\,dx \tag{29}$$

Only the integration of (25a) is performed here. From the definition of b_{1n} in (25a), and $\phi_{j+1}(x)$ in (16a):

$$b_{1n}=\frac{1}{h\sinh(2\omega_n h)}\int_{-h}^{+h} e^{-Bh}[a_{j+1}\,e^{Ax}+xb_{j+1}\,e^{-Ax}+(c_{j+1}-a_{j+1})\,e^{-Ax}]\sin[\alpha_n(x+h)]\,dx \tag{30}$$

Since ϕ will eventually be evaluated at the origin, (x_i, y_j), only the $n=$odd terms of the series in (24) and (25) need be considered. This allows considerable simplification of the expression for b_{1n}. The substitution of the expression for a_{j+1}, b_{j+1} and c_{j+1} from (13) and writing the exponential functions in terms of hyperbolic functions leads to the following:

for $n=$odd

$$b_{1n}=\frac{h\alpha_n\exp(-Bh)}{\sinh(2\psi_n h)[(Ah)^2+(\alpha_n h)^2]}\left(2\bar{\phi}_{i,j+1}\cosh(Ah)+\ldots\left[\frac{2Ah\cosh(Ah)}{(Ah)^2+(\alpha_n h)^2}-\sinh(Ah)\right]\right.$$
$$\left.\times[\bar{\phi}_{i+1,j+1}-\bar{\phi}_{i-1,j+1}-(\bar{\phi}_{i+1,j+1}+\bar{\phi}_{i-1,j+1})\coth(Ah)]\right) \tag{31}$$

Similar expressions are obtained for b_{2n}, b_{3n} and b_{4n} in terms of nodes on the other three boundaries.

Substituting the expression for b_{1n} from (30) into the expression for ϕ_1 from (24a) and evaluating ϕ_1 at (x_i, y_j) gives the desired result. Introducing the infinite series E_1 and E_2 and the constants A_1, A_2 and A_3 gives:

$$(\phi_1)_{i,j}=h\exp(-Bh)[\bar{\phi}_{i+1,j+1}A_1+\bar{\phi}_{i-1,j+1}A_2+\bar{\phi}_{i,j+1}A_3] \tag{32}$$

where,

$$A_1=\exp(-Ah)[(E_1/2)-E_2Ah\coth(Ah)]$$
$$A_2=A_1\exp(+2Ah)$$
$$A_3=2E_2[Ah\cosh(Ah)\coth(Ah)]$$

$$E_1 = \sum_{n=1,3,\ldots}^{\infty} \frac{(-1)^{(n-1)/2}\alpha_n}{[(Ah)^2+(\alpha_n h)^2]\cosh(\omega_n h)}$$

$$E_2 = \sum_{n=1,3,\ldots}^{\infty} \frac{(-1)^{(n-1)/2}\alpha_n}{[(Ah)^2+(\alpha_n h)^2]^2\cosh(\psi_n h)}$$

$$\lambda_n = \alpha_n^2 = \left(\frac{n\pi}{2h}\right)^2 \qquad \text{where } n = 1, 2, 3, \ldots$$

$$\omega_n^2 = (\lambda_n + A^2 + B^2 C)/C$$

Similarly, the expression for the ϕ_2 component problem becomes:

$$(\phi_2)_{i,j} = \mathrm{h}\exp(+Bh)[\bar{\phi}_{i+1,j-1}A_1 + \bar{\phi}_{i-1,j-1}A_2 + \bar{\phi}_{i,j-1}A_3] \tag{33}$$

The expressions for the ϕ_3 and ϕ_4 component problems are similar in form, but involve different series and constants,

$$(\phi_3)_{i,j} = h(-Ah)[\bar{\phi}_{i+1,j+1}B_1 + \bar{\phi}_{i+1,j-1}B_2 + \bar{\phi}_{i+1,j}B_3] \tag{34}$$

$$(\phi_4)_{i,j} = h(+Ah)[\bar{\phi}_{i-1,j+1}B_1 + \bar{\phi}_{i-1,j-1}B_2 + \bar{\phi}_{i-1,j}B_3] \tag{35}$$

where,

$$B_1 = \exp(-Bh)[(E_1'/2) - E_2' Bh\coth(Bh)]$$

$$B_2 = B_1\exp(+2Bh)$$

$$B_3 = 2E_2'[Bh\cosh(Bh)\coth(Bh)]$$

$$E_1' = \sum_{n=1,3,\ldots}^{\infty} \frac{(-1)^{(n-1)/2}\alpha_n}{[(Bh)^2+(\alpha_n h)^2]\cosh(\omega_n' h)}$$

$$E_2' = \sum_{n=1,3,\ldots}^{\infty} \frac{(-1)^{(n-1)/2}\alpha_n}{[(Bh)^2+(\alpha_n h)^2]^2\cosh(\omega_n' h)}$$

$$\frac{\lambda_n}{C} = \alpha_n^2 = \left(\frac{n\pi}{2h}\right)^2 \qquad \text{where } n = 1, 2, \ldots$$

$$(\omega_n')^2 = (\lambda_n + A^2 + B^2 C)$$

Finally, a solution for $\psi_{i,j}$ is obtained by noting that $\psi_{i,j} = \phi_{i,j}$ and using superposition of the four component problems,

$$\psi_{i,j} = \phi_{i,j} = \sum(\phi_n)_{i,j} \tag{36}$$

The expressions for the four component problems (ϕ_n) can be expressed in terms of the eight neighbouring ϕ nodes as in (32), (33), (34) and (35). Substituting for the ϕ nodes in terms of the ψ nodes results in the following equation:

$$\begin{aligned}\psi_{i,j} = h[&C_{i-1,j+1}\psi_{i-1,j+1} + C_{i,j+1}\psi_{i,j+1} + C_{i+1,j+1}\psi_{i+1,j+1} + C_{i-1,j}\psi_{i-1,j} + C_{i+1,j}\psi_{i+1,j} \\ &+ C_{i-1,j-1}\psi_{i-1,j-1} + C_{i,j-1}\psi_{i,j-1} + C_{i+1,j-1}\psi_{i+1,j+1} + C_f f]\end{aligned} \tag{37}$$

where,

$$C_{i-1,j-1} = A_2\exp(-Bh) + B_1\exp(+Ah)$$

$$C_{i,j+1} = A_3\exp(-Bh)$$

$$C_{i+1,j+1} = A_1\exp(-Bh) + B_1\exp(-Ah)$$

$$C_{i-1,j} = B_3\exp(+Ah)$$

$$C_{i+1,j} = B_3\exp(-Ah)$$

$$C_{i-1,j-1}=A_2\exp(+Bh)+B_2\exp(+Ah)$$

$$C_{i,j-1}=A_3\exp(+Bh)$$

$$C_{i+1,j-1}=A_1\exp(+Bh)+B_2\exp(-Ah)$$

$$C_f=h[A(C_{i+1,j+1}+C_{i+1,j-1}+C_{i+1,j}-(C_{i-1,j+1}+C_{i-1,j-1}+C_{i-1,j}))+B(C_{i+1,j+1}+C_{i-1,j+1}+C_{i,j+1}-(C_{i+1,j-1}+C_{i-1,j-1}+C_{i,j+1})]/(2(A^2+B^2C))$$

Equation (37) for $\psi_{i,j}$ is the locally analytic solution of the inhomogeneous, governing elliptic differential equation, (10). Note that the coefficients for ψ depend on the constants A_1, A_2, A_3, B_1, B_2 and B_3 which in turn depend on the infinite series E_1, E_2, E_1' and E_2'. This implies that if the coefficients of the governing equation, namely A, B and C, change then these series will have to be computed.

Stream function first derivative solutions

The derivatives of the solution for ψ are evaluated analytically, as opposed to a finite difference approximation. The differentiation is performed on the variables ϕ and $\bar{\phi}$ defined in (11). For convenience in describing this procedure, differentiation is performed individually on each of the four subproblems for ϕ defined in (12) and (20). Only the first derivatives of $\bar{\phi}_1$ will be calculated, the other component problem derivatives being similar.

Equation (11) and the definition of ϕ_1 from (24a) leads to the following:

$$\frac{\partial\bar{\phi}_1}{\partial x}=A\bar{\phi}_1+\exp(Ax+By)\sum_{n=1}^{\infty}b_{1n}\sinh[\omega_n(y+h)]\cos[\alpha_n(x+h)]\alpha_n \tag{38a}$$

$$\frac{\partial\bar{\phi}_1}{\partial y}=B\bar{\phi}_1+\exp(Ax+By)\sum_{n=1}^{\infty}b_{1n}\sin[\alpha_n(x+h)]\cosh[\omega_n(y+h)]\omega_n \tag{38b}$$

Evaluating at the origin causes all terms involving the cosine function to drop out because the index of summation ranges over only odd values. Thus at the origin:

$$\frac{\partial\bar{\phi}_1(x_i,y_j)}{\partial x}=A\bar{\phi}_1(x_i,y_j) \tag{39a}$$

$$\frac{\partial\bar{\phi}_1(x_i,y_j)}{\partial y}=B\bar{\phi}_1(x_i,y_j)+\sum_{n=1,3,\ldots}^{\infty}b_{1n}\sin[\alpha_nh]\cosh[\omega_nh]\omega_n \tag{39b}$$

The series summation on (39b) can be evaluated using the expression for b_{1n} in (31) and hyperbolic function identities. Introducing the infinite series G_1 and G_2 and the constants A_1', A_2' and A_3' gives the following:

$$\sum_{n=1,3,\ldots}^{\infty}b_{1n}\sin[\alpha_nh]\cosh[\omega_nh]\omega_n=h\exp(-Bh)[\bar{\phi}_{i+1,j+1}A_1'+\bar{\phi}_{i-1,j+1}A_2'+\bar{\phi}_{i,j+1}A_3'] \tag{40}$$

where,

$$A_1'=\exp(-Ah)[(G_1/2)-G_2Ah\coth(Ah)]$$

$$A_2'=A_1'\exp(+2Ah)$$

$$A_3'=2G_2[Ah\cosh(Ah)\coth(Ah)]$$

$$G_1=\sum_{n=1,3,\ldots}^{\infty}\frac{(-1)^{(n-1)/2}\alpha_n\omega_n}{[(Ah)^2+(\alpha_nh)^2]\sinh(\omega_nh)}$$

$$G_2=\sum_{n=1,3,\ldots}^{\infty}\frac{(-1)^{(n-1)/2}\alpha_n\omega_n}{[(Ah)^2+(\alpha_nh)^2]^2\sinh(\omega_nh)}$$

$$\lambda_n=\alpha_n^2=\left(\frac{n\pi}{2h}\right)^2 \qquad \text{where } n=1, 2, 3, \ldots$$

$$\omega_n^2=(\lambda_n+A^2+B^2C)/C$$

Similarly, the expression for ϕ_2 component problem becomes:

$$\frac{\partial\bar{\phi}_2(x_i, y_i)}{\partial x}=A\bar{\phi}_2(x_i, y_j) \tag{41a}$$

$$\frac{\partial\bar{\phi}_2(x_i, y_j)}{\partial y}=B\bar{\phi}_2(x_i, y_j)+\sum_{n=1,3,\ldots}^{\infty} b_{2n}\sin[\alpha_n h]\cosh[\omega_n h]\omega_n \tag{41b}$$

where,

$$\sum_{n=1,3,\ldots}^{\infty} b_{2n}\sin[\alpha_n h]\cosh[\omega_n h]\omega_n=-h(x)(+Bh)[\bar{\phi}_{i+1,j-1}A'_1+\bar{\phi}_{i-1,j-1}A'_2+\bar{\phi}_{i,j-1}A'_3]$$

The expressions for the ϕ_2 and ϕ_3 component problems are similar in form, but involve different constants,

$$\frac{\partial\bar{\phi}_3(x_i, y_j)}{\partial x}=A\bar{\phi}_3(x_i, y_j)+h\exp(-Ah)[\bar{\phi}_{i+1,j+1}B'_1+\bar{\phi}_{i+1,j-1}B'_2+\bar{\phi}_{i+1,j}B'_3] \tag{42a}$$

$$\frac{\partial\bar{\phi}_3(x_i, y_j)}{\partial y}=B\bar{\phi}_3(x_i, y_j) \tag{42b}$$

$$\frac{\partial\bar{\phi}_4(x_i, y_j)}{\partial x}=A\bar{\phi}_4(x_i, y_j)-h\exp(+Ah)[\bar{\phi}_{i-1,j+1}B'_1+\bar{\phi}_{i-1,j-1}B'_2+\bar{\phi}_{i-1,j}B'_3] \tag{42c}$$

$$\frac{\partial\bar{\phi}_4(x_i, y_j)}{\partial y}=B\bar{\phi}_4(x_i, y_j) \tag{42d}$$

where,

$$B'_1=\exp(-Bh)[(G'_1/2)-G'_2Bh\coth(Bh)]$$

$$B'_2=B'_1\exp(+2Bh)$$

$$B'_3=2G'_2[Bh\cosh(Bh)\coth(Bh)]$$

$$G'_1=\sum_{n=1,3,\ldots}^{\infty}\frac{(-1)^{(n-1)/2}\alpha_n\omega'_n}{[(Bh)^2+(\alpha_n h)^2]\sinh(\omega'_n h)}$$

$$G'_2=\sum_{n=1,3,\ldots}^{\infty}\frac{(-1)^{(n-1)/2}\alpha_n\omega'_n}{[(Bh)^2+(\alpha_n h)^2]^2\sinh(\omega'_n h)}$$

$$\frac{\lambda_n}{C}=\alpha_n^2=\left(\frac{n\pi}{2h}\right)^2 \qquad \text{where } n=1, 2, 3, \ldots$$

$$\omega'^2_n=(\lambda_n+A^2+B^2C)/C$$

The G-type series can be expressed in closed form. Defining $\bar{\phi}$ as a constant or linear function allows exact expressions for derivatives to be equated with expressions based on the G-type series,

$$G_1=\frac{B}{2h\sinh(Bh)\cosh(Ah)} \tag{43a}$$

$$G_1' = \frac{A}{2h \sinh(Ah) \cosh(Bh)} \tag{43b}$$

$$G_2 = \frac{A + h[B^2 C \tanh(Ah) - AB \coth(Bh)]}{4h^3 ABC \sinh(Bh) \cosh(Ah)} \tag{43c}$$

$$G_2' = \frac{BC + h[A^2 \tanh(Bh) - ABC \coth(Ah)]}{4h^3 AB \sinh(Ah) \cosh(Bh)} \tag{43d}$$

Expressions for the first derivative of ψ can now be obtained by differentiating the definition of $\bar{\phi}$ in (11),

$$\frac{\partial \psi}{\partial x} = \frac{\partial \bar{\phi}}{\partial x} - \frac{fA}{2(A^2 + B^2 C)} \tag{44a}$$

$$\frac{\partial \psi}{\partial y} = \frac{\partial \bar{\phi}}{\partial y} - \frac{fB}{2(A^2 + B^2 C)} \tag{44b}$$

Evaluating these expressions at the origin and substituting for $\bar{\phi}$ nodes in terms of ψ nodes results in the following expression for the x derivative,

$$\frac{\partial \psi}{\partial x}(x_i, y_j) = A\psi(x_i, y_j) + h[C^x_{i-1,j+1}\psi_{i-1,j+1} + C^x_{i+1,j+1}\psi_{i+1,j+1} + C^x_{i-1,j}\psi_{i-1,j} + C^x_{i+1,j}\psi_{i+1,j} + C^x_{i-1,j-1}\psi_{i-1,j-1} + C^x_{i+1,j-1}\psi_{i+1,j-1} + C^x_f f] \tag{45}$$

where,

$$C^x_{i-1,j+1} = -B_1' \exp(+Ah)$$
$$C^x_{i+1,j+1} = +B_1' \exp(-Ah)$$
$$C^x_{i-1,j} = -B_3' \exp(+Ah)$$
$$C^x_{i+1,j} = +B_3' \exp(-Ah)$$
$$C^x_{i-1,j-1} = -B_2' \exp(+Ah)$$
$$C^x_{i+1,j-1} = +B_2' \exp(-Ah)$$
$$C^x_f = [h\{B_1'(A \cosh(Ah) - B \sinh(Ah)) + B_2'(A \cosh(Ah) + B \sinh(Ah)) + B_3'(A \cosh(Ah))\} - A/(2h)]/(A^2 + B^2 C)$$

The expression for the y derivative is similar,

$$\frac{\partial \psi}{\partial y}(x_i, y_j) = B\psi(x_i, y_j) + h[C^y_{i-1,j+1}\psi_{i-1,j+1} + C^y_{i,j+1}\psi_{i,j+1} + C^y_{i+1,j+1}\psi_{i+1,j+1} + C^y_{i-1,j-1}\psi_{i-1,j-1} + C^y_{i,j-1}\psi_{i,j-1} + C^y_{i+1,j-1}\psi_{i+1,j-1} + C^y_f f] \tag{46}$$

where,

$$C^y_{i-1,j+1} = +A_2' \exp(-Bh)$$
$$C^y_{i,j+1} = +A_3' \exp(-Bh)$$
$$C^y_{i+1,j+1} = +A_1' \exp(-Bh)$$
$$C^y_{i-1,j-1} = -A_2' \exp(+Bh)$$
$$C^y_{i,j-1} = -A_3' \exp(+Bh)$$
$$C^y_{i+1,j-1} = -A_1' \exp(+Bh)$$

$$C_f^y = [h\{A_1'(B\cosh(Bh) - A\sinh(Bh)) + A_2'(B\cosh(Bh) + A\,\mathrm{snh}(Bh)) + A_3'(B\cosh(Bh))\} - B/(2g)]/(A^2 + B^2C)$$

The solution for ψ must be obtained before these derivatives can be evaluated.

Stream function cross derivative solution

The expression for the cross derivative builds on the expressions for the first derivatives. Combining (11) enables ψ and ϕ to be related,

$$\psi = \phi\exp(Ax+By) - \frac{f(Ax+By)}{2(A^2+B^2C)} \tag{47}$$

Taking the cross derivative of this equation and substituting for ϕ and its first derivatives in terms of $\bar{\phi}$ and its first derivatives leads to the following:

$$\frac{\partial^2\psi}{\partial x\partial y} = \exp(Ax+By)\left[AB\phi + A\frac{\partial\phi}{\partial y} + B\frac{\partial\phi}{\partial x} + \frac{\partial^2\phi}{\partial x\partial y}\right] \tag{48a}$$

$$\frac{\partial^2\psi}{\partial x\partial y} = AB\bar{\phi} + A\left[\frac{\partial\bar{\phi}}{\partial y} - B\bar{\phi}\right] + B\left[\frac{\partial\bar{\phi}}{\partial x} - A\bar{\phi}\right] + \exp(Ax+By)\frac{\partial^2\phi}{\partial x\partial y} \tag{48b}$$

$$\frac{\partial^2\psi}{\partial x\partial y} = A\frac{\partial\bar{\phi}}{\partial y} + B\frac{\partial\bar{\phi}}{\partial x} - AB\bar{\phi} + \exp(Ax+By)\frac{\partial^2\phi}{\partial x\partial y} \tag{48c}$$

Evaluating (48c) at the origin and expressing the first derivatives in terms of the constants defined in the previous section leads to:

$$\begin{aligned}\frac{\partial^2\psi}{\partial x\partial y}(x_i, y_j) = {} & A\{B\bar{\phi}(x_i, y_j) + h\exp(-Bh)[\bar{\phi}_{i+1,j+1}A_1' + \bar{\phi}_{i-1,j+1}A_2' + \bar{\phi}_{i,j+1}A_3']\ldots\} \\ & \times\{\ldots - h\exp(+Bh)[\bar{\phi}_{i+1,j-1}A_1' + \bar{\phi}_{i-1,j-1}A_2' + \bar{\phi}_{i,j-1}A_3']\} \\ & + B\{A\bar{\phi}(x_i, y_j) + h\exp(-Ah)[\bar{\phi}_{i+1,j+1}B_1' + \bar{\phi}_{i+1,j-1}B_2' + \bar{\phi}_{i+1,j}B_3']\ldots\} \\ & \times\{\ldots - h\exp(+Ah)[\bar{\phi}_{i-1,j+1}B_1' + \bar{\phi}_{i-1,j-1}B_2' + \bar{\phi}_{i-1,j}B_3']\} \\ & - AB\bar{\phi}(x_i, y_j) + \frac{\partial^2\phi}{\partial x\partial y}(x_i, y_j)\end{aligned} \tag{49}$$

All of the above terms except the cross derivative of ϕ were developed into coefficient form in the previous section. These previous results lead to:

$$\frac{\partial^2\psi}{\partial x\partial y}(x_i, y_j) = AB\bar{\phi}(x_i, y_j) + A\sum_{i,j} C_{i,j}^y\bar{\phi}_{i,j} + B\sum_{i,j} C_{i,j}^x\bar{\phi}_{i,j} + \frac{\partial^2\phi}{\partial x\partial y}(x_i, y_j) \tag{50}$$

The cross derivatives of ϕ are obtained by differentiating the expressions for the four component problems defined in (51). Only the cross derivatives of ϕ_1 will be calculated, the other component problem derivatives are similar,

$$\phi_1 = \sum_{n=1}^{\infty} b_{1n}\xi_{1n}\eta_{1n} = \sum_{n=1}^{\infty} b_{1n}\sin[\alpha_n(x+h)]\sinh[\omega_n(y+h)] \tag{51}$$

$$\frac{\partial^2\phi_1}{\partial x\partial y} = \sum_{n=1}^{\infty} b_{1n}\cos[\alpha_n(x+h)]\cosh[\omega_n(y+h)]\alpha_n\omega_n$$

Since (51) is evaluated at the origin, only n = even terms need be considered. Using the definition of b_{1n} from (30):

for n=even

$$b_{1n}=\frac{h\alpha_n \exp(-Bh)}{\sinh(2\omega_n h)[(Ah)^2+(\alpha_n h)^2]}\left(\bar{\phi}_{i+1,j+1}(-\exp(-Ah))\left[1+\frac{2Ah}{(Ah)^2+(\alpha_n j)^2}\right]\cdots\right.$$
$$\left.+\bar{\phi}_{i-1,j+1}\exp(+Ah)\left[1-\frac{2Ah}{(Ah)^2+(\alpha_n h)^2}\right]+2\bar{\phi}_{i,j+1}\left[\frac{2Ah\cosh(Ah)}{(Ah)^2+(\alpha_n h)^2}\right]\right) \quad (52)$$

Similar expressions are obtained for b_{2n}, b_{3n} and b_{4n} in terms of nodes on the other three boundaries.

Placing the expression for b_{1n} from (52) into (51) and evaluating at the origin, (x_i, y_j), gives the desired result. Introducing the infinite series K_1 and K_2 and the constants L_1, L_2 and L_3 gives:

$$\frac{\partial^2\phi_1}{\partial x\partial y}(x_i, y_j)=h\exp(-Bh)[\bar{\phi}_{i+1,j+1}L_1+\bar{\phi}_{i-1,j+1}L_2+\bar{\phi}_{,j+1}L_3] \quad (53)$$

where,

$$L_1=-\exp(-Ah)[K_{1/2}+K_2Ah]$$
$$L_2=\exp(+Ah)[K_{1/2}-K_2Ah]$$
$$L_3=2Ah\cosh(Ah)K_2$$
$$K_1=\sum_{n=2,4,\ldots}^{\infty}\frac{(-1)^{n/2}\alpha_n^2\omega_n}{[(Ah)^2+(\alpha_n h)^2]\sinh(\omega_n h)}$$
$$K_2=\sum_{n=2,4,\ldots}^{\infty}\frac{(-1)^{n/2}\alpha_n^2\omega_n}{[(Ah)^2+(\alpha_n h)^2]^2\sinh(\omega_n h)}$$
$$\lambda_n=\alpha_n^2=\left(\frac{n\pi}{2h}\right)^2 \qquad \text{where } n=1, 2, 3, \ldots$$
$$\omega_n^2=(\lambda_n+A^2+B^2C)/C$$

Similarly, the expression for the ϕ_2 component problem becomes:

$$\frac{\partial^2\phi_2}{\partial x\partial y}(x_i, y_j)=-h\exp(+Bh)[\bar{\phi}_{i+1,j-1}L_1+\bar{\phi}_{i-1,j-1}L_2+\bar{\phi}_{i,j-1}L_3] \quad (54)$$

The expressions for the ϕ_3 and ϕ_4 component problems are similar in form, but involve different series and constants,

$$\frac{\partial^2\phi_3}{\partial x\partial y}(x_i, y_j)=h\exp(-Ah)[\bar{\phi}_{i+1,j+1}L_1'+\bar{\phi}_{i+1,j-1}L_2'+\bar{\phi}_{i+1,j}L_3'] \quad (55)$$

$$\frac{\partial^2\phi_4}{\partial x\partial y}(x_i, y_j)=-h\exp(+Ah)[\bar{\phi}_{i-1,j+1}L_1'+\bar{\phi}_{i-1,j-1}L_2'+\bar{\phi}_{i-1,j}L_3'] \quad (56)$$

where,

$$L_1'=-\exp(-Bh)[K_{1/2}'+K_2'Bh]$$
$$L_2'=\exp(+Bh)[K_{1/2}'-K_2'Bh]$$
$$L_3'=2Bh\cosh(Bh)K_2'$$
$$K_1'=\sum_{n=2,4,\ldots}^{\infty}\frac{(-1)^{n/2}\alpha_n^2\omega_n'}{[(Bh)^2+(\alpha_n h)^2]\sinh(\omega_n' h)}$$

$$K'_2 = \sum_{n=2,4,\ldots}^{\infty} \frac{(-1)^{n/2}\alpha_n^2\omega'_n}{[(Bh)^2+(\alpha_n h)^2]^2 \sinh(\omega'_n h)}$$

$$\frac{\lambda_n}{C} = \alpha_n^2 = \left(\frac{n\pi}{2h}\right)^2 \qquad \text{where } n = 1, 2, 3, \ldots$$

$$(\omega'_n)^2 = (\lambda_n + A^2 + B^2 C)$$

Substituting these results for the cross derivative of ϕ, noting that $\psi_{i,j} = \phi_{i,j}$, and substituting for $\bar{\phi}$ nodes in terms of ψ nodes gives the desired result,

$$\frac{\partial^2\psi}{\partial x \partial y}(x_i, y_j) = AB\psi(x_i, y_j) + h[C^{xy}_{i-1,j+1}\psi_{i-1,j-1} + C^{xy}_{i,j+1} + C^{xy}_{i+1,j+1}\psi_{i+1,j+1} + \cdots$$
$$+ C^{xy}_{i-1,j}\psi_{i-1,j} + C^{xy}_{i+1,j}\psi_{i+1,j} + C^{xy}_{i-1,j-1}\psi_{i-1,j-1} + C^{xy}_{i,j-1}\psi_{i,j-1}$$
$$+ C^{xy}_{i+1,j-1}\psi_{i+1,j-1} + C^{xy}_f f] \tag{57}$$

where,

$$C^{xy}_{i-1,j+1} = AC^y_{i-1,j+1} + BC^x_{i-1,j+1} + L_2\exp(-Bh) - L'_1\exp(+Ah)$$
$$C^{xy}_{i,j+1} = AC^y_{i,j+1} + L_3\exp(-Bh)$$
$$C^{xy}_{i+1,j+1} = AC^y_{i+1,j+1} + BC^x_{i+1,j+1} + L_1\exp(-Bh) + L'_1\exp(-Ah)$$
$$C^{xy}_{i-1,j} = BC^x_{i-1,j} - L'_3\exp(+Ah)$$
$$C^{xy}_{i+1,j} = BC^x_{i+1,j} + L'_3\exp(-Ah)$$
$$C^{xy}_{i-1,j-1} = AC^y_{i-1,j-1} + BC^x_{i-1,j-1} - L_2\exp(+Bh) - L'_2\exp(+Ah)$$
$$C^{xy}_{i,j-1} = AC^y_{i,j-1} - L_3\exp(+Bh)$$
$$C^{xy}_{i+1,j-1} = AC^y_{i+1,j-1} + BC^x_{i+1,j-1} - L_1\exp(+Bh) + L'_2\exp(-Ah)$$
$$C^{xy}_f = h[A(C^{xy}_{i+1,j+1} + C^{xy}_{i+1,j-1} + C^{xy}_{i+1,j} - (C^{xy}_{i-1,j+1} + C^{xy}_{i-1,j-1} + C^{xy}_{i-1,j}))$$
$$+ B(C^{xy}_{i+1,j+1} + C^{xy}_{i-1,j+1} + C^{xy}_{i,j+1} - (C^{xy}_{i+1,j-1} + C^{xy}_{i-1,j-1} + C^{xy}_{i,j-1}))]/(2(A^2 + B^2C))$$

and the $C^x_{i,j}$ and $C^y_{i,j}$ coefficients are given by (45) and (46).

The solution for ψ must be obtained before the cross derivative can be evaluated.

Initialization procedure

An analytical one-dimensional flow field is used to begin the iteration procedure. The specified exit pressure ratio (p_{back}/P_0) is used to calculate the exit velocity, mass flux, and critical area ratio. A back pressure ratio of 0.53 is used for a highly compressible flow, with a back pressure of 0.99 for nearly incompressible flow. The following relationships which are exact for the uniform flow at the inlet and outlet, are used to initialize the flow,

$$M^2 = \frac{2}{\gamma - 1}\left[\left(\frac{p}{P_0}\right)^{(1-\gamma)/\gamma} - 1\right] \tag{58}$$

$$\hat{u}^2 = \left(\frac{u}{a^*}\right)^2 = \frac{(\gamma+1)M^2}{2+(\gamma-1)M^2} \tag{59}$$

$$\hat{\rho} = \frac{\rho}{\rho_0} = \left(\frac{p}{P_0}\right)^{1/\gamma} \tag{60}$$

$$\frac{A}{A^*} = \frac{1}{M}\left[\left(\frac{2}{\gamma+1}\right)\left(1 + \frac{\gamma-1}{2}M^2\right)\right]^{\gamma+1/2(\gamma-1)} \tag{61}$$

where M is the Mach number, A is the local cross sectional area of the nozzle, and A^* is the critical area.

Since the flow is isentropic, the critical area is constant and can be used to relate the local area and Mach number. Letting the subscript E denote the exit location where conditions are known:

$$A_E\left(\frac{A^*}{A}\right)_E - A\left(\frac{A^*}{A}\right) = 0 \tag{62}$$

where the critical area ratio is given as a function of Mach number in (58).

This nonlinear equation is solved for M with the secant method. The flow variables (u, p, ρ) are then defined in terms of M using (58), (59) and (60).

The one-dimensional flow field is used to construct an approximate ψ. The stream function is approximated by noting that the x-direction mass flow must be constant. The planar flowstream function is given in (63), with a similar relationship found for the axisymmetric stream function,

$$\psi = \int \frac{\partial \psi}{\partial y}\,dy = \int \rho u\,dy = \int \frac{\text{const}}{A}\,dy \tag{63}$$

For the velocity field to match the solid wall boundary condition, the y component of velocity, v, is also approximated. The streamwise derivative of ψ is approximated by finite differences and used to define v. The x component of velocity, u, is not changed. This quasi-two-dimensional flow field is used to start the locally analytical iteration procedure.

Iteration procedure

Once an approximation to the flow field has been obtained, the coefficients of the stream equation, (1), can be evaluated. These coefficients, A, B and C, are then used to calculate the locally analytic nodal coefficients, $C_{i,j}$, for the iteration procedure. This procedure consists of two nested loops, denoted the inner and outer loop. In the inner iteration loop, a point successive over relaxation (SOR) scheme is used, with the relaxation factor, r, being specified by the user. The r factors used for the various grids in this investigation are given in *Table 1*.

The maximum residual, defined as $|\Delta\psi/\psi|$, is calculated during each SOR sweep. After each sweep the maximum residual is compared with a user specified tolerance, usually 10^{-5}. If the residual exceeds the tolerance another SOR sweep is performed, with a maximum of ten sweeps per inner iteration loop. If more than one SOR sweep is required, then the locally analytical coefficients are re-calculated and another inner iteration loop performed. The maximum number of these outer iteration loops is specified by the user. Iteration stops when the tolerance exceeds the maximum residual after one SOR sweep or the specified number of outer iteration loops are performed.

The Dirichlet boundary conditions for ψ cause difficulties in evaluating boundary derivatives. A locally analytical derivative evaluation requires that a node have all eight neighbours. Since this requirement is not met at the boundaries, one-sided second-order finite differences are used

Table 1 Over-relaxation factors, r, for various grids

Grid size	r
25 × 4	1.2
50 × 8	1.5
100 × 16	1.8

to evaluate the derivatives of ψ at the centre-line and wall. After this final step the solution is complete.

RESULTS

To demonstrate the modelling and locally analytical solution, this analysis is applied to predict the flow in convergent nozzles, both planar and axially symmetric, for different back pressures. Six nozzle configurations are considered, selected to demonstrate the effect of the grid, the nozzle geometry, and back pressure. These configurations are defined in *Table 2.*

This solution procedure was implemented as an approximately 1500 line FORTRAN program and executed on a Gould NP-1 minicomputer. The CPU times required to analyze the six nozzle configurations are given in *Table 2.* The CPU time required for execution was proportional to the deviation from the one-dimensional approximation used to initialize the flow. This is especially evident for the axisymmetric nozzle, Case 6. The CPU time decreased from Case 1 to Case 3 because fewer iterations were required to reach the same tolerance using the finer grid. A lower tolerance was used for the axisymmetric geometry because of a slower convergence rate.

Grid

The effect of grid refinement on the predicted Mach contours is demonstrated in *Figures 3* and *4* corresponding to Cases 1 and 2, respectively. As the grid is refined, the Mach contours become smoother, indicating a convergent solution.

The effect of grid refinement on the streamline patterns is shown in *Figures 5* and *6,* corresponding to Cases 1 and 3, respectively. For these fairly fine grids, no change in the streamline pattern is observed.

Table 2 Results for various grids, geometries, and back pressures

Case	Grid	p_{back}	Geometry	Tol.	CPU time (sec)	Study
1	50×8	0.53	planar	10^{-5}	0.8	Baseline
2	25×4	0.53	planar	10^{-5}	0.1	Grid
3	100×16	0.53	planar	10^{-5}	0.7	Grid
4	100×16	0.53	planar	10^{-6}	6.3	Tolerance
5	50×8	0.99	planar	10^{-5}	0.3	Back pressure
6	50×8	0.53	axisymmetric	10^{-4}	3.2	Geometry

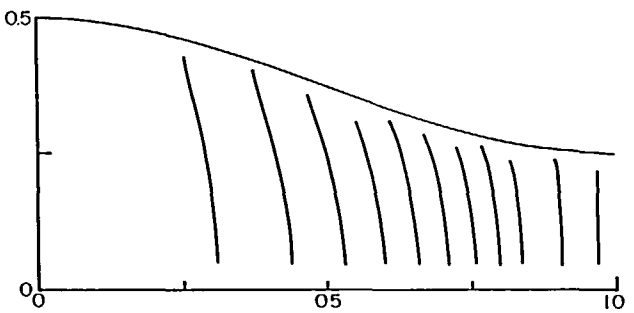

Figure 3 Case 1 planar nozzle Mach contours: 50×80 grid

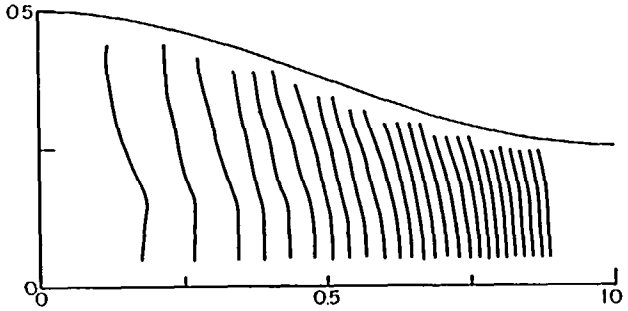

Figure 4 Case 2 planar nozzle Mach contours: 25 × 4 grid

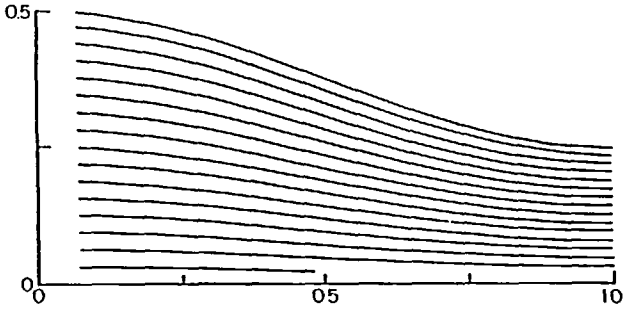

Figure 5 Case 1 planar nozzle streamlines: 50 × 80 grid

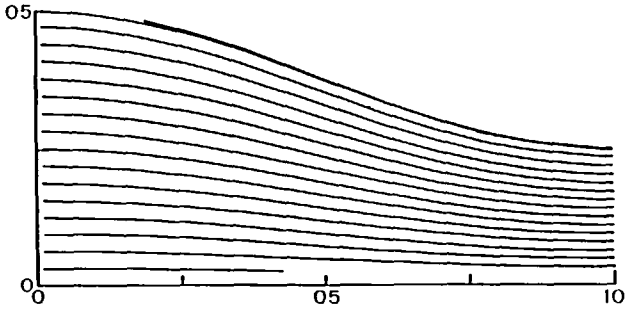

Figure 6 Case 3 planar nozzle streamlines: 100 × 16 grid

Tolerance

The effect of decreasing tolerance is shown by comparing Cases 3 and 4. Decreasing the tolerance by one order of magnitude increases the CPU time by approximately one order of magnitude.

Back pressure

The effect of back pressure on the Mach contours is demonstrated in *Figures 3* and *7*, corresponding to Cases 1 and 5, respectively. For the nearly incompressible case ($p_{back}/P_0 = 0.99$)

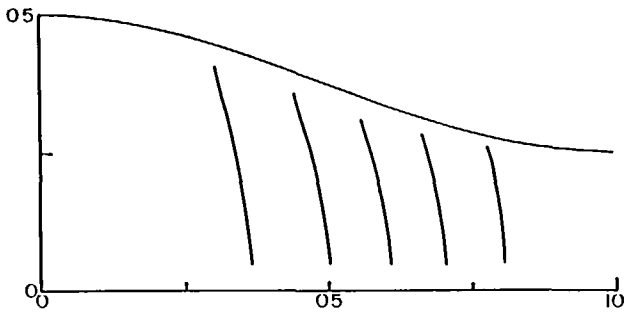

Figure 7 Case 5 planar nozzle Mach contours

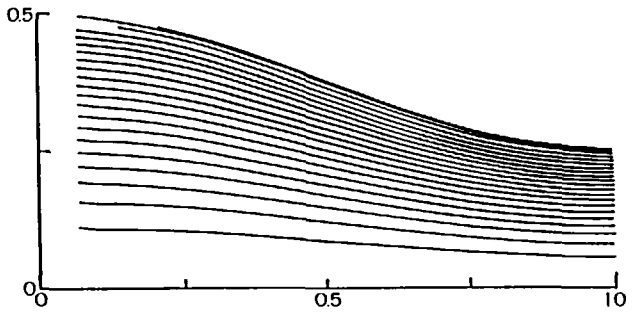

Figure 8 Case 6 axisymmetric nozzle streamlines

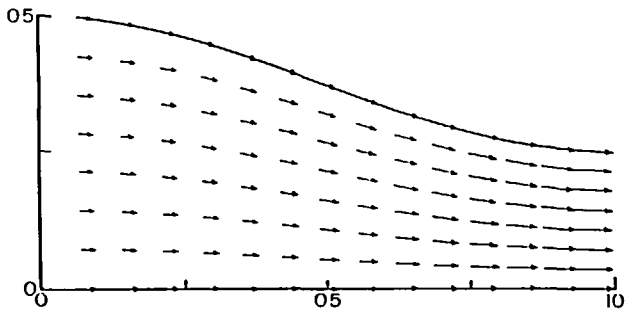

Figure 9 Case 1 planar nozzle velocity vectors

the maximum Mach number variation along any normal plane is approximately 7%. This variation can be interpreted as deviation from the one-dimensional flow approximation. For the compressible case ($p_{back}/P_0 = 0.53$), the maximum Mach number variation along any normal plane is approximately 10%. The variation is greater for the lower back pressure because of compressibility effects.

Geometry

The effect of geometry on the streamline patterns is shown in *Figures 5* and *8*, corresponding to Cases 1 and 6, respectively. In both cases the streamlines smoothly relax from the curved

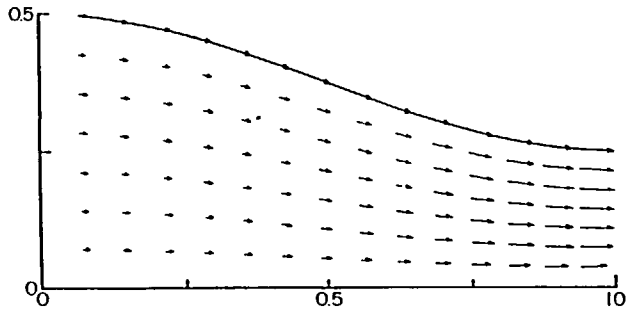

Figure 10 Case 6 axisymmetric velocity vectors

contour of the nozzle wall to the straight contour of the centre-line. There are dramatic differences between the planar and axially symmetric streamline patterns. The axisymmetric streamlines crowd together as y increases because the cross sectional area is proportional to y^2, as opposed to y for the planar streamlines.

The effect of geometry on the velocity vectors is shown in *Figures 9* and *10*, corresponding to Cases 1 and 6, respectively. In both cases the velocity magnitude increases with decreasing area as expected from conservation of mass. The direction of the velocity vectors varies smoothly from tangent at the nozzle wall to straight along the centre-line. The increase in velocity magnitude through the nozzle was greater for axisymmetric flow than for planar symmetric flow because of the greater convective acceleration.

CONCLUSIONS

This paper has presented the first compressible flow solution based solely on the locally analytical method, accomplished by developing the flow model and locally analytical solution for inviscid subsonic compressible flow. The stream function for irrotational, compressible flow without body forces was chosen as the governing differential equation. The governing equations were developed in a form amenable to numerical solution. The stream function for irrotational, compressible flow without body forces was chosen as the governing differential equation. With the simplifying assumptions made, the remaining governing equations reduced to algebraic equations. The modelling and locally analytical solution was then demonstrated by applying this analysis to predict the flow in convergent nozzles, both planar and axially symmetric, for different back pressures.

The locally analytical solution for the steady, isentropic, subsonic flow through a converging nozzle is somewhat slower[1] than the finite difference method, but promises more accurate results as it is based on an analytical solution. Further development is necessary to extend this solution method to more complex flow geometries.

REFERENCES

1 Chen, C. J., Naseri-Nashat, H. and Ho, K. S. Finite analytic numerical solution of heat transfer in two-dimensional cavity flow, *J. Num. Heat Transfer*, 4, 179–197 (1981)
2 Chen, C. J. and Li, P. Finite differential methods in heat conduction—Application of analytic solution techniques, *ASME Paper 79-WA/HT-50* (1979)
3 Ching-Jen Chen and Chen, Wen-Chung, The finite analytic method, Vol. 7, *Iowa Institute of Hydraulic Res. Rep. No. 232-VII*, University of Iowa, Iowa City, Iowa (1984)
4 Chen Naixing, Weihong, Li and Xiadodong Chen, A new approach for solving blade cascade flow by using the finite analytic solution method, *ASME Paper 86-GT-109* (1986)
5 Ching-Jen Chen and Chen, Hamn-Ching, The finite analytic method, Vol. 4, *Iowa Institute of Hydraulic Res. Rep. No. 232-IV*, University of Iowa, Iowa City, Iowa (1982)